

## Fundamental two-electron tensor-operator description of the $Gd^{3+} 4f^7$ configuration exchange splittings in $GdCl_3\uparrow$

R. S. Meltzer

*Department of Physics and Astronomy, University of Georgia, Athens, Georgia 30602*

R. L. Cone

*Department of Physics and Astronomy, University of Georgia, Athens, Georgia 30602  
and Department of Physics, Montana State University, Bozeman, Montana 59715\**

(Received 23 April 1975)

The applicability and usefulness of a fundamental two-electron description of the exchange interaction in magnetic rare-earth insulators, has been tested by applying it in spherical tensor-operator form to the analysis of the observed exchange splittings of  $GdCl_3$ . The experimental splittings were obtained by extrapolating the optical transition energies from the ground state to five excited levels as a function of large magnetic fields back to zero field, thereby determining the splittings in a nearly completely ordered  $Gd^{3+}$  environment. An analysis of the mechanisms which can give rise to the splittings shows that only the exchange and magnetic dipole-dipole interactions can contribute. The contributions from the latter and from the dynamic exchange, which we show must be included in the analysis of the  $\vec{k} = 0$  exciton exchange splittings in concentrated materials, are isolated, allowing the determination of the static exchange contribution. An analysis of the selection rules on the exchange Hamiltonian in this host for the states of the  ${}^6P$  manifold allows us to eliminate all but two parameters in the two-electron exchange operator which is applied to the observed static exchange contributions. The two parameters were determined from data on five exciton states and the resulting isotropic parameter is shown to be identical to that determined from magnetic studies of the ground state. Further studies indicate that the fitted two-electron exchange parameters are applicable not only to other levels of  $Gd^{3+}$  in  $GdCl_3$ , but also to those of other rare-earth ions.

### I. INTRODUCTION

For problems involving exchange interactions between ions in both the ground state and a number of excited states, it is desirable to use a formulation of the exchange interaction which not only provides an adequate description for each state but also allows the exchange matrix elements for different states to be related theoretically. The effective-spin-Hamiltonian method clearly provides an adequate and quite successful description for the limited group of states spanned by the effective spin, but unfortunately the empirical parameters are, in general, not directly applicable to other states.

The simplest form of coupling between *real* spins is the isotropic exchange  $-2J\vec{S}_1 \cdot \vec{S}_2$ , but this form of interaction has been shown to be inadequate for describing many experimental observations.<sup>1-3</sup> The reason for its inadequacy in the general case is that the exchange interaction is fundamentally an interaction between individual pairs of electrons. The "two-electron" exchange integrals<sup>9</sup> which describe this interaction generally depend upon the orbital states of the electrons, and this orbital dependence leads to an *inherent anisotropy* in the interaction.<sup>1,2,7,8</sup> When the orbital dependence is taken into account, there may be as many as 1225 different "two-electron" exchange

integrals for problems involving rare-earth ions. Symmetry fortunately reduces this number in most cases. Even so, experimental determination of all the remaining exchange integrals would seem to present an intractable problem.

A major simplification arises, however, when it is noted that in some cases, only a *few recurrent linear combinations* of "two-electron" exchange integrals are required for a complete description of specific phenomena. It is then feasible to experimentally determine these linear combinations and to readily calculate the relationships between exchange matrix elements for different ionic states, making it possible to *predict* results for other electronic levels. Indeed, as we have shown in an earlier letter,<sup>4</sup> the calculated relationships may be *independent* of experimental parameters in favorable cases.

The simplification regarding the number of experimental parameters is most apparent when the exchange interaction is expressed directly in terms of the real orbital and spin angular momenta of the ions involved. The basis for applying this approach has been provided by the two-electron spherical tensor operator formulation developed by Levy<sup>7</sup> and Elliott and Thorpe.<sup>8</sup> The parameters involved in the theory are just the linear combinations of two-electron exchange integrals mentioned above. Moreover, the power-

ful tensor operator methods are well suited to multielectron calculations, particularly by computer.

We have already applied this approach successfully to the transfer-of-energy exchange interaction which is responsible for the exciton dispersion in  $\text{GdCl}_3$ ,<sup>4</sup> Cone and Wolf<sup>3</sup> have used this method to relate the exchange splittings of  $\text{Er}^{3+}$  impurity levels in ferromagnetic  $\text{Tb}(\text{OH})_3$ , and Levy,<sup>10</sup> Orlich and Hufner,<sup>11</sup> and Dean *et al.*<sup>12</sup> have applied it to exchange splittings of  $\text{Er}^{3+}$  in erbium iron garnet. More recently, Meltzer and Cone<sup>13</sup> have studied the systematic variations of the orbitally dependent exchange parameters in  $\text{GdCl}_3$  using the exchange splittings of  $\text{Nd}^{3+}$  and  $\text{Er}^{3+}$  impurities.

The purpose of the present paper is to extend the earlier analysis in  $\text{GdCl}_3$  to describe the exchange splittings as well as the dispersion of the exciton levels. The isotropic and relevant anisotropic exchange parameters have been determined from the excited-state data. A striking test of the success of this description of the exchange interaction is the agreement between the isotropic parameter determined from the excited-state analysis with that of the ground-state measurements by Clover and Wolf<sup>14</sup> based on a study of the high-frequency susceptibility.

In Sec. II we apply the two-electron spherical tensor operator formulation of the exchange interaction to the exciton states of  $\text{GdCl}_3$ . We describe the experimental determination of the exchange splittings in Sec. III. In Sec. IV we determine the  $\text{GdCl}_3$  two-electron exchange parameters from the observed spectra and compare the isotropic parameter determined from the optical data with that determined from high-frequency susceptibility studies of the ground state. In Sec. V the important conclusions are summarized and suggestions are made for extending the method to other systems.

## II. THEORY OF EXCITON LEVEL SPLITTINGS

In the simplest cases, particularly those involving impurities, the single-ion model involving an "exchange field"<sup>15</sup> or a much more general exchange potential<sup>3</sup> has been useful in the description of exchange splittings. In a pure crystal such as  $\text{GdCl}_3$ , however, Frenkel excitons rather than crystal single-ion product states are the true eigenstates of the system due to the translational symmetry and resonant interionic coupling. Meltzer and Moos<sup>16</sup> have in fact shown that the excitonic nature of the states in  $\text{GdCl}_3$  has important effects on the observed optical spectrum.

The purpose of Sec. II is to separate the non-dispersive and dispersive contributions to the observed splittings and to apply the tensor operator theory to the  $\vec{k}=0$  exciton states, thereby enabling the *true* experimental exchange splittings in excited states to be related theoretically. In Sec. II A the exciton states for ferromagnetic  $\text{GdCl}_3$  are described. The interaction matrix in the  $\vec{k}=0$  sublattice exciton representation is derived for the case in which all matrix elements coupling excitons derived from different single-ion states are ignored. (This assumption is justified in Sec. II B.) The matrix elements consist of two classes: the so-called "static" matrix elements which are  $\vec{k}$  independent and are responsible for the band shift and the "dynamic" matrix elements which lead to energy transfer and dispersion. In the present case of  $\text{GdCl}_3$ , the band shift and dispersion are shown to give simply additive contributions to the experimentally observed energy separation between the  $\vec{k}=0$  excitons arising from a single-ion Kramers doublet. These separations are often called "exchange splittings" in magnetic systems although the magnetic dipole-dipole interaction, and in some cases the electric multipole interactions, may give significant contributions to the total splitting. Since the dynamic matrix elements have been previously determined from line-shape studies, the dynamic contribution to the splittings may be simply subtracted from the experimentally observed splittings to yield the static contribution.

In Sec. II B the various mechanisms for the interionic interactions are considered, and it is shown that only the exchange and magnetic dipole-dipole interactions are expected to give important contributions. In Sec. II C the two-electron tensor operator exchange Hamiltonian is described and applied with the results of Sec. II A to the exchange interactions between the nearest and next-nearest neighbors in  $\text{GdCl}_3$ . It is shown that the exchange splittings of several excited states can be related to one another *and* to the exchange splitting of the ground state.

### A. Exciton representation and the interaction matrix

We start with single-ion states whose Hamiltonian includes the free-ion terms, the crystal field, and the Zeeman interactions. For almost all states of interest in the present analysis,  $J$  and  $M_J$  remain good quantum numbers.<sup>17</sup> In intermediate coupling the single-ion states are expressed as linear combinations of the form

$$|J, M_J\rangle = \sum_{S, L} \alpha(S, L, J) |S, L, J, M_J\rangle \approx |\mu\rangle, \quad (1)$$

where  $\mu$  identifies the single-ion state and the  $\alpha(S, L, J)$  are coefficients which have been described previously.<sup>18</sup> The crystal field for  $\text{GdCl}_3$  has been discussed by Schwiesow and Crosswhite.<sup>19</sup> In all experiments to be discussed here, the external magnetic field lies along the hexagonal  $c$  axis, so the Zeeman term takes the form

$$\mathcal{H}_{\text{Zeeman}} = -\mu_B(L_z + 2S_z)H_z, \quad (2)$$

where  $\mu_B$  is the Bohr magneton,  $L_z$  and  $S_z$  are the  $z$  components of the total orbital and spin angular momenta, and  $H_z$  is the applied field.

The interactions between the  $\text{Gd}^{3+}$  ions are described by the Hamiltonian

$$V = \sum'_{i(p), j(q)} V_{i(p)j(q)}, \quad (3)$$

where  $i$  and  $j$  label ions on sublattices  $p$  and  $q$  and where the prime signifies that all ion pairs are to be included in the sum only once. To determine the crystal eigenstates of this Hamiltonian we begin by forming translationally invariant Bloch waves from products of the single-ion states. These are defined for the two sublattices in  $\text{GdCl}_3$  by

$$|\mu_{\vec{k}, p}\rangle = N^{-1/2} \sum_i e^{-i\vec{k} \cdot \vec{T}_{i(p)}} |\mu_{i(p)}\rangle, \quad (4)$$

where  $N$  is the number of unit cells,  $\vec{k}$  is a reciprocal-lattice vector, and  $\vec{T}_{i(p)}$  is the pure lattice translation connecting the origin to the  $p$ th ion of the  $i$ th unit cell. The state  $|\mu_{i(p)}\rangle$  denotes the  $N$ -ion product state

$$|\mu_{i(p)}\rangle = |e_{i(p)}^\mu\rangle \prod_{j(p) \neq i(p)} |g_{j(p)}\rangle, \quad (5)$$

where  $e_{i(p)}^\mu$  denotes the ion  $i(p)$  in excited state  $\mu$  and  $g_{j(p)}$  denotes ion  $j(p)$  in the ground state ( ${}^8S_{7/2}, M_J = -7/2$ ).

Each single-ion state  $\mu$  thus gives two degenerate sublattice states for each of the  $N$  values of  $\vec{k}$ .<sup>20</sup> The transfer-of-energy interaction couples these Bloch waves, forming two exciton branches in  $k$  space from each single-ion state. Meltzer and Moos<sup>16</sup> have given the transformation which diagonalizes the transfer-of-energy Hamiltonian and the resulting eigenvalues. The energy dispersion was found to be up to  $1 \text{ cm}^{-1}$  in the states within the  ${}^6P$  manifold of  $\text{GdCl}_3$  and as large as  $2 \text{ cm}^{-1}$  in the isostructural compound  $\text{Gd}(\text{OH})_3$ ; hence, it makes an important contribution to the measured exchange splittings.

We are primarily interested in the  $\vec{k}=0$  excitons as these are the ones which are observed in optical transitions from the ground state. The matrix of the interaction Hamiltonian is now formed in

the  $\vec{k}=0$  sublattice representation. All matrix elements coupling excitons derived from different single-ion states  $\mu$  are ignored. This approximation is justified in Sec. II B. Thus each single-ion state gives rise to a  $2 \times 2$  matrix

$$\mathcal{H}_{\text{exch}} = \begin{pmatrix} W^\mu + V_{11}^\mu & V_{12}^\mu \\ V_{12}^\mu & W^\mu + V_{11}^\mu \end{pmatrix}, \quad (6)$$

where

$$W^\mu = \sum_{j(q)} \langle e_{i(p)}^\mu g_{j(q)} | V_{i(p)j(q)} | e_{i(p)}^\mu g_{j(q)} \rangle; \quad j(q) \neq i(p) \quad (7)$$

is the static part of the interaction responsible for the band shift,

$$V_{11}^\mu = \sum_{i'} \langle e_{i(p)}^\mu g_{i'(p)} | V_{i(p)i'(p)} | g_{i(p)} e_{i'(p)}^\mu \rangle; \quad i \neq i' \quad (8)$$

is the dynamic part of the interaction responsible for energy transfer between ions on the same sublattice,<sup>21</sup> and

$$V_{12}^\mu = \sum_j \langle e_{i(p)}^\mu g_{j(q)} | V_{i(p)j(q)} | g_{i(p)} e_{j(q)}^\mu \rangle; \quad p \neq q \quad (9)$$

is the dynamic contribution of the interaction responsible for energy transfer between ions on opposite sublattices.<sup>21</sup>

This matrix is essentially identical to that derived by Meltzer and Moos<sup>16</sup> except that it is specialized to the  $\vec{k}=0$  excitons and includes explicitly the band shift  $W^\mu$ . When the sum in Eq. (8) is restricted to the two nearest neighbors with energy transfer matrix elements  $v_1^\mu$  and the sum in Eq. (9) is restricted to the six next-nearest neighbors with energy transfer matrix elements  $v_2^\mu$  the  $2 \times 2$  matrix becomes

$$\mathcal{H}_{\text{exch}} = \begin{pmatrix} W^\mu + 2v_1^\mu & 6v_2^\mu \\ 6v_2^\mu & W^\mu + 2v_1^\mu \end{pmatrix}. \quad (10)$$

A sum over neighbors is still implicit in  $W^\mu$ . The resulting eigenvalues are

$$E^\mu(\pm) = W^\mu + 2v_1^\mu \pm 6|v_2^\mu|. \quad (11)$$

Transitions from the ground state are allowed to the  $\vec{k}=0$  excitons which are even (+) [odd(-)] under inversion for magnetic [electric] dipole transitions. The observed splittings thus correspond to the energy difference between the even [odd]  $\vec{k}=0$  excitons arising from the two single-ion components within a Kramers doublet. Labeling these two states  $+\mu$  and  $-\mu$  and noting that for a Kramers pair of states

$$W^{+\mu} = -W^{-\mu} \equiv W^{\mu}, \quad (12)$$

the exchange splitting is

$$\Delta E^{\text{MD[ED]}} = 2W^{\mu} + 2(v_1^{+\mu} - v_1^{-\mu}) + [-]6(|v_2^{+\mu}| - |v_2^{-\mu}|) \quad (13)$$

where the brackets refer to the case of electric dipole transitions. For  $\text{GdCl}_3$  the dynamic contributions for the upper components of the Kramers pairs are zero<sup>22</sup>; hence, Eq. (13) can be written

$$\Delta E^{\text{MD[ED]}} = 2W^{\mu} - 2v_1^{-\mu} - [+ ]6|v_2^{-\mu}|. \quad (14)$$

Thus, the contributions of the static and dynamic matrix elements are simply added to give the total observed "exchange splittings." As a result, the previously determined<sup>16</sup> dynamic terms may be subtracted directly from the observed splittings to isolate the static contributions for analysis.

The roles played by these two types of interionic coupling are shown schematically in Fig. 1. The static terms destroy the Kramers degeneracy, the external field further increases the splitting, and the dynamic terms produce a  $\vec{k}$  dependence of the exciton energy. The transitions from the  $\vec{k}=0$  ground state are shown by the vertical arrows. The observed splittings for the case of magnetic dipole ( $\Delta E^{\text{MD}}$ ) and electric dipole transitions ( $\Delta E^{\text{ED}}$ ) are shown on the right. It can be seen that the total observed splitting includes a contribution from the dynamic terms.

Since the dynamic terms may in principle be as large as or even larger than the static terms, they should clearly be considered in any analysis of the exchange splittings. In determining whether the dynamic terms contribute one must be particularly careful to note that large exciton affects can become manifest in a variety of ways. For transitions involving the simultaneous creation of two excitons or for those occurring between two exciton bands, the exciton affects are revealed directly in the line shapes since  $\vec{k}$  can be conserved for all points in the Brillouin zone. Examples of these two-exciton processes which have revealed significant energy dispersions in rare-earth systems are the magnon-exciton optical absorption in  $\text{GdCl}_3$ ,<sup>16</sup> the band-to-band fluorescence observed in  $\text{Tb}(\text{OH})_3$ ,<sup>23</sup> and the band-to-band light scattering in  $\text{PrAlO}_3$ .<sup>24</sup> When a single exciton process occurs for which the initial or final state is the ground state, the presence of exciton dispersion will not appear in the line shape, but rather in the factor group or Davydov splitting of the  $\vec{k}=0$  excitons. Such splittings have been observed in several transition-metal magnetic insulators such as  $^{25}\text{Cr}_2\text{O}_3$  and in the rare-earth orthochromites,<sup>26</sup> but they have not

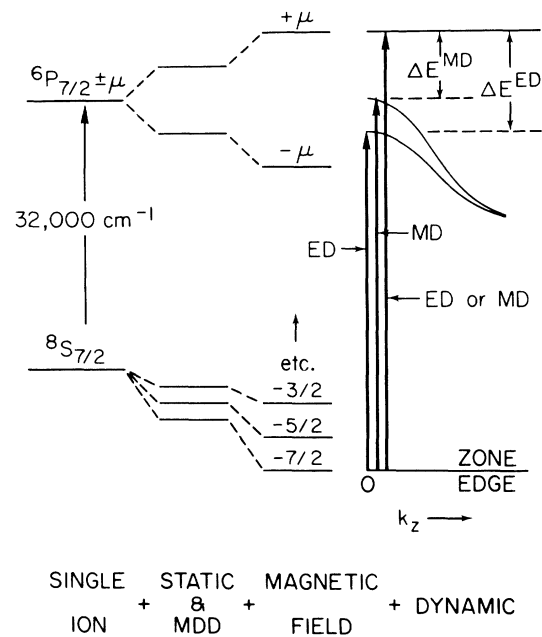


FIG. 1. Illustration of the contributions to the splitting of a Kramers pair. The splittings of the  $\vec{k}=0$  excitons for magnetic dipole transitions  $\Delta E^{\text{MD}}$  and electric dipole transitions  $\Delta E^{\text{ED}}$  are shown to contain a contribution from the dynamic part of the exchange interaction.

to our knowledge been observed in rare-earth systems. In  $\text{GdCl}_3$ , the selection rules forbid optical transitions from the ground state to one of the two  $\vec{k}=0$  excitons so that the factor group splitting cannot be observed. The evidence for exciton dispersion was derived instead from band-to-band transitions from the magnon band. Thus, in  $\text{GdCl}_3$  the evidence for significant dynamic contributions to the exchange splittings is not an outstanding feature of the optical spectrum, but must be carefully extracted. Care must therefore be exercised in drawing conclusions in other concentrated rare-earth systems.

#### B. Contributions of the interionic interactions to the exciton matrix elements

The static and dynamic matrix elements discussed above may in general contain contributions from electronic exchange, the magnetic dipole-dipole interaction (MDD), the static electric multipole-multipole interaction (EMI), and the induced EMI resulting from an exchange of virtual phonons (VPE). Reviews of these mechanisms have been given by Wolf<sup>1</sup> and Baker.<sup>2</sup> In an earlier letter<sup>4</sup> we showed that only anisotropic exchange contributed to the dynamic terms. In this section it is shown that only exchange and MDD can contribute to the static splittings in  $\text{GdCl}_3$ , as was

found to be the case in a similar analysis of impurity level splittings by Cone and Wolf.<sup>3</sup> The MDD and exchange contributions are simply additive when the matrix elements  $W^\mu$  of Eq. (7) are evaluated. Thus, by accurately calculating the static MDD contributions, it is possible to isolate the static exchange contributions. Details of the analysis are considered for each of the interactions below.

### 1. Electronic exchange interaction

In order to provide an adequate description of the exchange interaction between electrons on neighboring ions, the orbital dependence of the exchange is taken into account by writing for the exchange Hamiltonian

$$\mathfrak{H}_{\text{exch}} = \sum_{a,b} -\mathcal{J}(m_a m_b; m'_a m'_b) (\frac{1}{2} + 2\vec{s}_a \cdot \vec{s}_b), \quad (15)$$

where the summations are over the electrons on ion  $i(p)$  and the electrons on ion  $j(q)$ . [The labels  $i(p)$  and  $j(q)$  for the ions are omitted here for brevity.] Both two-center or direct exchange and three-center or superexchange processes involving the ligands are considered to contribute to the integrals  $\mathcal{J}(m_a m_b; m'_a m'_b)$ . Except for relationships derived from symmetry, the 1225  $\mathcal{J}$ 's are independent. Minimal requirements for the validity of Eq. (15) would be dominance of a particular electronic configuration in the states of interest and negligible effects due to higher-order permutations.

As we pointed out in the Introduction, application of the above expression to many problems is *greatly simplified* by the fact that only a fraction of the total number of exchange constants are relevant to a description of specific phenomena. Moreover, for  $\text{GdCl}_3$  and a number of other realistic systems, only a *few recurrent* linear combinations are required.

This is most easily demonstrated by exploiting the symmetry of the multielectron states of the individual ions resulting from the much larger "free-ion" and crystal field single-ion terms. Elliott and Thorpe<sup>8</sup> and Levy<sup>7</sup> have rewritten the above exchange interaction in a *different but completely equivalent* form which is well-suited to this approach. The exchange constants are expanded in terms of irreducible spherical tensor operators which act in the orbital spaces of the individual electrons on the respective ions and which have well-defined symmetry properties given by the representations  $\underline{D}^{(k)}$  of the full rotation group.

The exchange Hamiltonian for a pair of ions is then written

$$\mathfrak{H}_{\text{exch}} = - \sum_{a,b} \sum_{k,k'} \sum_{q,q'} \Gamma_{qq'}^{kk'} u_q^{(k)}(a) u_q^{(k')}(b) (\frac{1}{2} + 2\vec{s}_a \cdot \vec{s}_b), \quad (16)$$

where the  $\Gamma_{qq'}^{kk'}$  are linear combinations of the two electron exchange integrals<sup>4</sup>:

$$\Gamma_{qq'}^{kk'} = \sum_{m_a, m'_a} \sum_{m_b, m'_b} (-1)^{m_a + m_b} \begin{pmatrix} l & k & l \\ -m_a & q & m_a' \end{pmatrix} \begin{pmatrix} l & k' & l \\ -m_b & q' & m_b' \end{pmatrix} \times \mathcal{J}(m_a m_b; m'_a m'_b). \quad (17)$$

[The quantities in large parentheses in Eq. (17) are the usual 3-j symbols.] The  $u_q^{(k)}$  are the spherical tensor operators which act in the orbital spaces of the individual electrons and are defined<sup>27</sup> by

$$(l || u^{(k)} || l) = (2k+1)^{1/2}. \quad (18)$$

As before  $\vec{s}$  is the spin angular momentum operator for a single electron, and the summations over  $a$  and  $b$  include the electrons on ions  $i(p)$  and  $j(q)$ , respectively. The remaining summations are over the ranks  $k$  and components  $q$  of the orbital operators, where  $k, k' \leq 2l$ . The  $\Gamma_{00}^{00}$  term is the usual isotropic Heisenberg exchange as we show in Sec. IV. Terms with  $k$  or  $k'$  nonzero are anisotropic. Our earlier work<sup>4</sup> on dynamic exchange in  $\text{GdCl}_3$  has demonstrated that the  $k, k' \neq 0$  terms may be as large as the isotropic term in rare-earth systems.

The requirements of time reversal symmetry and a Hermitian energy matrix give

$$(\Gamma_{qq'}^{kk'})^* = (-1)^{q+q'} \Gamma_{-q-q'}^{kk'} \quad (19)$$

and

$$k+k' \text{ even}. \quad (20)$$

There are of course as many independent  $\Gamma_{qq'}^{kk'}$  as there are  $\mathcal{J}(m_a m_b; m'_a m'_b)$ ; however, as we shall see below, the symmetry of the  $\text{Gd}^{3+}$  states dramatically reduces the number of  $\Gamma_{qq'}^{kk'}$  relevant to the present analysis although the number of  $\mathcal{J}$ 's involved is still quite large. The advantage of Eq. (16) over Eq. (15) for the empirical analysis of experimental data is thus quite striking. We wish to emphasize again, however, that Eq. (16) is *completely equivalent* to Eq. (15).

In  $\text{GdCl}_3$ , the nearest-neighbor (nn)  $\text{Gd}^{3+}$  ions are situated adjacent to each other on the  $c$  axis as shown in Fig. 2. The pair symmetry is  $C_{3h}$  with the  $\sigma_h$  reflection plane perpendicular to the  $c$  axis and passing through the intervening triad of  $\text{Cl}^-$  ions. Application of the  $\sigma_h$  and  $c_3$  operations respectively gives

$$\Gamma_{qq'}^{kk'}(\text{nn}) = (-1)^{q+q'} \Gamma_{q'q}^{k'k}(\text{nn}) \quad (21)$$

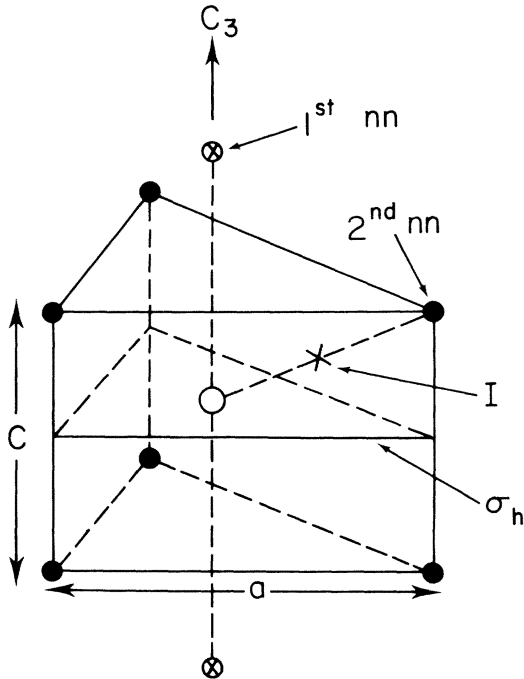


FIG. 2. Crystal structure of  $\text{GdCl}_3$  showing a unit cell, the 1st and 2nd nearest neighbor  $\text{Gd}^{3+}$  ions, and some of the symmetry operations of the lattice used in determining the form of the exchange Hamiltonian.

and

$$q + q' = 0, \pm 3, \pm 6, \pm 9, \pm 12. \quad (22)$$

Each  $\text{Gd}^{3+}$  ion has six next-nearest neighbors (nnn) located in triads  $\frac{1}{2}c$  above and below it. The only symmetry operation for these pairs other than the identity operation is the inversion operator  $I$  acting through a point halfway along the line joining the two ions. This gives

$$\Gamma_{qq'}^{kk'}(\text{nnn}) = \Gamma_{q'q}^{k'k}(\text{nnn}). \quad (23)$$

No specific restrictions on  $q$  and  $q'$  result from this operation.

Both the static and dynamic terms involve a summation over neighbors. The two-electron exchange parameters  $\Gamma_{qq'}^{kk'}$  for the two nearest neighbors are related by applying the  $\sigma_h$  operation through the central  $\text{Gd}^{3+}$  ion. Those of the six nnn are related by applying the  $C_{3h}$  operations about the central  $\text{Gd}^{3+}$  ion. When these operations are carried out and the various contributions of the different neighbors summed, only terms with  $q + q' = 0, \pm 6, \pm 12$  give nonzero contributions for either type neighbor and for either static or dynamic matrix elements. This is a quite general result for the  $\text{GdCl}_3$ -type crystal structure and does not depend on the  $\text{Gd}^{3+}$  states; nevertheless, a relatively large number of parameters remain.

The most dramatic reduction in the number of parameters results from consideration of the symmetry of the  $\text{Gd}^{3+}$  states of interest, and in this case different results are obtained for static and dynamic terms. We consider first the static matrix elements, which are of the form

$$\langle e_{i(\rho)}^u g_{j(q)} | V_{i(\rho)j(q)} | e_{i(\rho)}^u g_{j(q)} \rangle. \quad (24)$$

The intermediate coupling free-ion wave functions for  $\text{Gd}^{3+}$  indicate that the  ${}^8S_{7/2}$  ground state and  ${}^6P_J$  excited states are essentially pure with only slight admixtures of  ${}^6P$  and  ${}^6D$ , respectively.<sup>18</sup> For pure  ${}^8S$  and  ${}^6P$  states only the real terms  $\Gamma_{00}^{00}$  (isotropic) and  $\Gamma_{00}^{20}$  (anisotropic) contribute to the static matrix elements. The terms with  $k' = 1$  are eliminated by the requirement of  $k + k'$  even; moreover, Cone and Wolf<sup>3</sup> and Levy<sup>10</sup> have shown that only even  $k$  terms need to be considered in the analysis of static splittings. The  ${}^6D$  admixture into  ${}^6P_J$  allows a contribution by  $\Gamma_{00}^{40}$  but there is a reduction of its contribution by a factor of 0.13 due to the admixture coefficients. Other terms allowed by admixtures into  ${}^8S_{7/2}$  or  ${}^6P_J$  are reduced by factors of 0.02 even in the most favorable cases. Barring the possibility that the additional  $\Gamma_{qq'}^{kk'}$  themselves are significantly larger than those allowed for the pure states and considering the present experimental accuracy, it is quite reasonable to ignore all terms except  $\Gamma_{00}^{00}$  and  $\Gamma_{00}^{20}$  in evaluating the static matrix elements for  $\text{GdCl}_3$ . Since only two exchange parameters must be determined from data on five observed levels, the internal consistency of the analysis provides a test of this conclusion.

Using the same assumption of essentially pure  ${}^8S_{7/2}$  and  ${}^6P_J$  states, we have concluded in an earlier letter<sup>4</sup> that the anisotropic terms  $\Gamma_{-1}^{11} = \Gamma_{-11}^{11}$  and  $\Gamma_{00}^{11}$  make the dominant contributions to the dynamic matrix elements for nearest neighbors. Both are real and their values are  $\Gamma_{-1}^{11}(\text{nn}) = 0.28 \pm 0.05 \text{ cm}^{-1}$  and  $\Gamma_{00}^{11}(\text{nn}) = 0.14 \pm 0.07 \text{ cm}^{-1}$ . The data for next-nearest-neighbor dynamic matrix elements which are smaller and have large relative uncertainties do not allow firm conclusions to be drawn in that case, although the same terms would be expected to dominate. (For either type of neighbor, reduction factors of 0.13 apply to the  $\Gamma_{qq'}^{22}$  dynamic contribution due to the small calculated  ${}^6D$  admixture coefficients.<sup>18</sup>) This model for nearest neighbors involving only the  $k = k' = 1$  terms predicts the ratios of a number of dynamic matrix elements independent of the values of the parameters, so the excellent agreement of the predicted and observed ratios provides strong evidence for this interpretation.

We now consider the dynamic and static exchange contributions to "off-diagonal" matrix

elements of the form

$$\langle g_{i(p)} e_{j(q)}^{\mu} | V_{i(p)j(q)} | e_{i(p)}^{\mu'} g_{j(q)} \rangle \quad (25)$$

or

$$\langle e_{i(p)}^{\mu} g_{j(q)} | V_{i(p)j(q)} | e_{i(p)}^{\mu'} g_{j(q)} \rangle, \quad (26)$$

where  $e^{\mu}$  and  $e^{\mu'}$  represent different excited states. As the  $L$  values for the states of interest limit  $k, k' \leq 4$  even with  ${}^6D$  admixtures,  $q + q' = 0$  for the exchange interaction. Whether static or dynamic terms are considered, this requires that  $M_J = M'_J$  for the two excited states. Since such states are in different  $J$  manifolds, coupling of excitons by such terms is completely negligible<sup>28</sup> in this system. It should be noted in particular that the two single-ion components of a Kramers doublet cannot be coupled.

Off-diagonal matrix elements of the form

$$\langle g_{i(p)} e_{j(q)}^{\mu} | V_{i(p)j(q)} | e_{i(p)}^{\mu'} g'_{j(q)} \rangle \quad (27)$$

or

$$\langle e_{i(p)}^{\mu} g_{j(q)} | V_{i(p)j(q)} | e_{i(p)}^{\mu'} g'_{j(q)} \rangle, \quad (28)$$

where  $e^{\mu}$  and  $e^{\mu'}$  may be the same or different and where  $g'$  represents a spin deviation, could seriously affect the analysis of Sec. IIA at low fields, but their contributions are reduced at the higher fields used in the analysis of Sec. IV. Further discussion of the fields and temperatures required to eliminate the effects of such terms is given in Sec. IV.

### 2. Magnetic dipole-dipole interaction

Unlike the other interactions, the MDD interaction may be accurately calculated. Therefore its contribution to the observed splittings can be easily determined. The static terms may be calculated using the magnetic moments for  $Gd^{3+}$  in the various excited states determined from Zeeman effect measurements and the known dipolar field  $H_{dip}$ :

$$W_{dip}^{\mu} = -\mu_z H_{dip}, \quad (29)$$

where  $H_{dip}$  is computed from the known magnetic moment of the ground state, the crystal structure, and the demagnetizing factor for the crystal.

In our earlier analysis of dynamic matrix elements<sup>4</sup> we concluded that the dynamic MDD contribution was negligible compared to that of the anisotropic exchange. The same is true for off-diagonal terms of the type described in Sec. I above, although other MDD matrix elements involving only  ${}^8S_{7/2}$  states do play a role in admixing spin deviations into the ground state.

### 3. Electric multipole interaction and virtual phonon exchange

The static terms provided by the EMI impart equal band shifts to each of the excitons arising from the components of a single-ion Kramers doublet in a first-order analysis, thus giving no contribution to the splittings.<sup>3</sup> Higher-order contributions by EMI in  $GdCl_3$  could arise only from the electric quadrupole-quadrupole coupling (EQQ) due to the small orbital angular momenta involved for the states of interest. As a result of the unusual properties of the half filled  $4f^7$  shell under charge conjugation,<sup>18</sup> even EQQ requires the admixture of both  ${}^6P$  and  ${}^6D$  into the ground state as well as admixture of  ${}^6D$  into the excited state. Comparison of  $Gd^{3+}$  EQQ static matrix elements with those for  $Ce^{3+}$  which are on the order of  $2 \text{ cm}^{-1}$  in the rare-earth trihalides,<sup>2</sup> reveals a reduction by  $10^{-3}$ ; hence, EQQ contributions to the splittings via higher-order processes are entirely negligible in  $GdCl_3$ .

As we pointed out in our earlier analysis of the dynamic terms,<sup>4</sup> the EMI makes a negligible contribution to the dispersion. The off-diagonal EMI matrix elements are also negligible.

Since the VPE interaction has the same form as the EMI, similar reduction factors apply to its contributions; moreover, the energy denominator dependence of the VPE coefficients<sup>2,23</sup> effectively rules out a large contribution for the highly excited  ${}^6P_J$  states.

### III. EXPERIMENTAL DETERMINATION OF THE ZERO-FIELD EXCHANGE SPLITTINGS

In order to facilitate a theoretical description of the "exchange splittings" of  $GdCl_3$ , we wish to determine the zero-field splittings under conditions in which all electronically unexcited  $Gd^{3+}$  ions are in a single well-defined state, the ferromagnetic ground state. It should be emphasized that for  $GdCl_3$  the difficulty of treating other experimental conditions arises strictly from many-body effects which we discuss below, *not* from limitations of our description of the exchange interaction.

A ferromagnetic crystal would clearly be in the ferromagnetic ground state at  $T = 0 \text{ K}$ , but at  $1.2 \text{ K}$ , the lowest temperature achievable in these optical experiments, higher levels of the  $Gd^{3+}$  spin system are significantly populated in a ferromagnet such as  $GdCl_3$  ( $T_c = 2.20 \text{ K}$ ) due to the relatively small magnon energy gap. These  $Gd^{3+}$  spin excitations broaden the optical transitions from the  ${}^8S_{7/2}$  manifold and produce unresolved exchange splittings, since the energy separations between the exchange split transitions are on the order of the linewidths due to the statistically varying in-

interactions between the excited  $Gd^{3+}$  ions and the "sea" of thermally populated neighboring spins.

Alternatively, one can study the exchange splittings in a strong external magnetic field which greatly reduces the linewidths at finite temperatures by driving the magnon branch up in energy, decreasing the magnon population and producing a well-aligned paramagnet. The exchange splittings are then found by extrapolating the high-field results to zero field. This technique, which was employed in our experiments, has several advantages. The observed exchange splittings result from the interaction of an electronically excited  $Gd^{3+}$  ion with a nearly perfectly aligned spin system, so that approximations concerning the relationships between the observed splittings and the average spin state of the  $Gd^{3+}$  environment are avoided. Moreover, the technique is also applicable to paramagnetic systems which do not order spontaneously at accessible temperatures.

The experiments were performed briefly as follows. Polarized absorption spectra of samples of  $GdCl_3$  were studied in fields up to 30 kG directed parallel to the  $c$  axis. The spectra were recorded photographically on a nine-meter Ebert spectrograph with a resolution of  $0.3 \text{ cm}^{-1}$ . The samples were grown from the melt using a Bridgeman technique.<sup>29</sup> Since the hygroscopic samples were sealed in quartz tubes under  $\frac{1}{2}$  an atmosphere of helium, they were not in direct thermal contact with the liquid helium bath. Therefore, to minimize the heat input to the sample, all absorption spectra were recorded using a  $50 \text{ \AA}$  bandpass continuum obtained with a low resolution monochromator placed between the AH-6 high-pressure mercury capillary lamp and the sample. The helium bath temperature was maintained at 1.2 K. Alignment of the samples was assured due to the strong torque exerted on the ferromagnetic crystals by the external field.

The nearly pure  $M_J$  character of the crystal field states in the  ${}^6P$  manifold presented serious problems in the experimental determination of the zero-field exchange splittings due to the restrictive selection rules for transitions from the  ${}^8S_{7/2}, M_J = -\frac{7}{2}$  ground state which are summarized in Table I. In the first and second columns are listed, respectively, the crystal quantum numbers  $\mu$ , which label the irreducible representations of the point group  $C_{3h}$ , and the major, and in parentheses, minor,  $M_J$  composition of the states. In Column 3 the selection rules for the  $M_J$  components comprising the crystal field state are described where that of the minor component is in parentheses. Here  $M$  and  $E$  signify magnetic and electric dipole transitions while  $\pi$  and  $\sigma$  indicate light polarized with the electric vector parallel

TABLE I. Calculated and observed selection rules for transitions from  ${}^8S_{7/2}, M_J = -\frac{7}{2}$  to the single-ion states in the  ${}^6P$  manifold.

Excited level $\mu$	$M_J$ <sup>a</sup>	Selection rules from ${}^8S_{7/2}, -\frac{7}{2}$			
		Calculated <sup>b</sup> All ${}^6P$ manifolds	${}^6P_{7/2}$	${}^6P_{5/2}$	${}^6P_{3/2}$
$\frac{5}{2}$	$-\frac{7}{2}(\frac{5}{2})$	$M\sigma$	...	$\sigma(\pi)$	
$-\frac{5}{2}$	$\frac{7}{2}(-\frac{5}{2})$	...	$(M\pi)$	$(\pi)$	
$-\frac{5}{2}$	$-\frac{5}{2}(\frac{7}{2})$	$M\pi$	...	$\pi$	$\pi$
$\frac{5}{2}$	$\frac{5}{2}(-\frac{7}{2})$	...	$(M\sigma)$	$(\sigma)$	...
$-\frac{3}{2}$	$-\frac{3}{2}$	$E\sigma$		$\sigma$	$\sigma$ $\sigma$
$\frac{3}{2}$	$\frac{3}{2}$	...		...	...
$-\frac{1}{2}$	$-\frac{1}{2}$	$E\pi$		$\pi(\sigma)$	$\pi(\sigma)$ $\pi(\sigma)$
$\frac{1}{2}$	$\frac{1}{2}$	$E\sigma$		$(\sigma)$	$(\sigma)$ $(\sigma)$

<sup>a</sup> The coefficient of the component in parentheses is very small for the  ${}^6P_J$  states.

<sup>b</sup> Selection rules in parentheses are those of the minor  $M_J$  component.

<sup>c</sup> Polarization in parentheses is observed only very weakly.

and perpendicular to the  $c$  axis. Columns 4–6 describe the observed spectra for the  $J = \frac{7}{2}, \frac{5}{2},$  and  $\frac{3}{2}$  manifolds, respectively. Parentheses signify that the transition in that polarization is very weak.

As can be seen from Table I, transitions to the  $M_J = +\frac{5}{2}$  and  $+\frac{7}{2}$  states are forbidden by either transition mechanism. Therefore the upper component of the  $\mu = \pm\frac{5}{2}$  Kramers doublets may be observed only by virtue of a small admixture of  $M_J = -\frac{7}{2}$  and  $-\frac{5}{2}$ , respectively. The  ${}^6P_{7/2}$  manifold contains both  $M_J = \pm\frac{7}{2}$  and  $M_J = \pm\frac{5}{2}$  states so both pairs of  $\mu = \pm\frac{5}{2}$  states have a slightly impure  $M_J$  character. As a result the upper component of each was observed in sufficiently thick samples. However, in thick samples the lower component is strongly overabsorbed in the allowed polarization, making it difficult to accurately locate its transition energy. It does, however, appear very weakly in the forbidden polarization, where its energy at all fields is identical, within experimental accuracy, with the transition energy of the allowed polarization. In the fitting procedure described below, data from both polarizations were included for the lower components. For the  ${}^6P_{5/2}$  manifold, there are no  $M_J = \pm\frac{7}{2}$  states so the  $\mu = \pm\frac{5}{2}$  states are essentially pure  $M_J = \pm\frac{5}{2}$ , especially as the  $600 \text{ cm}^{-1}$  energy difference from the  ${}^6P_{7/2}$  manifold is sufficient to make  $J$  mixing negligible. The upper transitions to  $\mu = +\frac{5}{2}$  were therefore not observable, and a determination of the  ${}^6P_{5/2} \mu = \pm\frac{5}{2}$  exchange splitting was impossible.



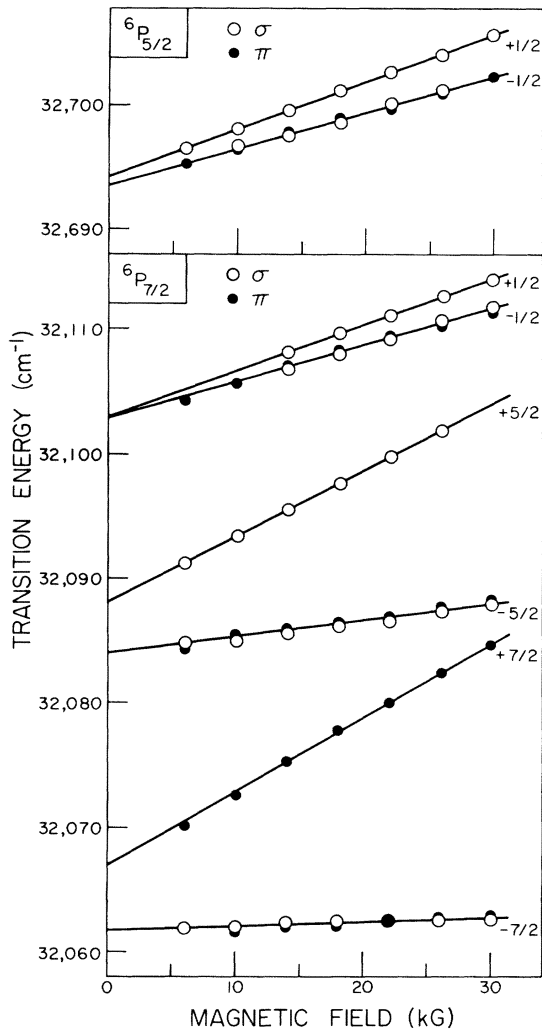


FIG. 3. Transition energies at 1.2 K of transitions from the ground state to the components of the  ${}^6P$  manifold as a function of applied magnetic field along the  $c$  axis. The dominant  $M_J$  value of the state is listed on the right-hand side.

This is particularly unfortunate as the coefficient of the  $\Gamma_{00}^{20}$  anisotropic term for this state is larger than that for any of the other  ${}^6P$  states as we shall see in Sec. IV.

The exchange splittings of the  $\mu = \pm \frac{3}{2}$  states in all three manifolds were not observable since the  $\mu = +\frac{3}{2}$  states are pure  $M_J = +\frac{3}{2}$ , and the transition to  $M_J = +\frac{5}{2}$  is forbidden (see Table I). Transitions to both components of the  $\mu = \pm \frac{1}{2}$  Kramers pairs of states are allowed so their splitting could be determined in all three manifolds. The transition to  $\mu = -\frac{1}{2}$  appears weakly in the forbidden polarization at the same energy as in the allowed polarization. In the analysis below, data from both polarizations were included.

It was shown in Sec. II that the dynamic and static contributions to the exchange splittings appear as separate terms along the diagonal of the exchange matrix in the  $\vec{k} = 0$  exciton representation. Since no significant "off-diagonal" matrix elements connect different  $\vec{k} = 0$  exciton states of the  ${}^6P_J$  manifolds, the dependence of transition energy on field should be linear in the aligned state. The exchange splittings were thus determined by extrapolating the observed transition energies to zero field.

The magnetic field dependence of the transition energies to some of the Kramers pairs of states in the  ${}^6P_{7/2}$  and  ${}^6P_{5/2}$  manifolds of  $\text{GdCl}_3$  at 1.2 K are shown in Fig. 3, where the solid lines are linear least-squares fits to the data between 14 and 30 kG. The nonlinear dependence on field below 14 kG results from the increasing population of spin deviations at lower fields.

The zero-field exchange splitting  $\Delta E_{\text{obs}}$  and  $g$ -factor  $g_{\text{obs}}$  of each Kramers pair were determined by performing a least-squares fit to the energy differences between the two components of the pair as a function of field. The results of these fits are given in Table II. The resulting values

TABLE II. Contributions to the observed exchange splittings of  $\text{Gd}^{3+}$  in  $\text{GdCl}_3$  and a calculated least-squares fit to the static contribution.

State	$\Delta E_{\text{obs}}$	$g_{\text{obs}}$	$g_{\text{calc}}$	$\Delta E_{\text{dyn}}^a$	$\Delta E_{\text{MDD}}^b$	$\Delta E_{\text{static}}^c$	$\Delta E_{\text{calc}}^d$
${}^6P_{7/2} \pm \frac{7}{2}$	$5.35 \pm 0.3$	5.92	5.85	$-0.30 \pm 0.2$	$1.57 \pm 0.1$	$4.08 \pm 0.6$	4.20
${}^6P_{7/2} \pm \frac{5}{2}$	$4.13 \pm 0.2$	4.31	4.18	$0.00 \pm 0.2$	$1.12 \pm 0.1$	$3.01 \pm 0.5$	2.87
${}^6P_{7/2} \pm \frac{1}{2}$	$0.17 \pm 0.5$	0.80	0.84	0	0.21	$-0.04 \pm 0.5$	0.55
${}^6P_{5/2} \pm \frac{1}{2}$	$0.76 \pm 0.7$	0.92	0.92	0	0.22	$0.54 \pm 0.7$	0.77
${}^6P_{3/2} \pm \frac{1}{2}$	$2.02 \pm 0.8$	1.16	1.16	0	0.03	$1.99 \pm 0.8$	1.20

<sup>a</sup> Contribution of dynamic exchange to observed splitting.

<sup>b</sup> Contribution of magnetic dipole-dipole interaction to observed splitting.

<sup>c</sup> Contribution of static exchange to observed splitting.  $\Delta E_{\text{static}} = \Delta E_{\text{obs}} - \Delta E_{\text{dyn}} - \Delta E_{\text{MDD}}$ .

<sup>d</sup> Contribution of static exchange calculated using fitted parameters shown in Eqs. (30) and (31).

of  $\Delta E_{\text{obs}}$  should be identical to the splittings at  $T = 0$  K since all data used in the least-squares fit was obtained in large fields at 1.2 K where  $\text{GdCl}_3$  is a well-aligned paramagnet.<sup>30</sup> The agreement between  $g_{\text{obs}}$  and  $g_{\text{calc}}$ , calculated on the basis of intermediate coupling wave functions,<sup>18</sup> is excellent.

The dynamic exchange  $\Delta E_{\text{dyn}}$  and magnetic dipole-dipole contributions  $\Delta E_{\text{MDD}}$  to the observed splittings are also shown in Table II. The former were determined from a line-shape analysis of band-to-band transitions from the magnon state.<sup>16</sup> The latter were obtained using the dipole field, which has been accurately calculated for  $\text{GdCl}_3$ ,<sup>31</sup> and the observed  $g$ -factors. The demagnetizing factors employed in the determination of the dipole field were those calculated at the center of the two rectangular samples used in this study.<sup>32</sup>

As we have shown in Sec. II, the zero-field splittings  $\Delta E_{\text{obs}}$  represent the simple algebraic sum of the magnetic dipole-dipole contribution and the static and dynamic exchange contributions to the splittings of the  $\vec{k} = 0$  excitons of a Kramers pair of states. The dynamic part of the exchange and the MDD contribution were thus subtracted from the observed splittings to yield the static exchange contribution  $\Delta E_{\text{static}}$ , which is also shown in Table II.

#### IV. EVALUATION OF THE TWO-ELECTRON EXCHANGE PARAMETERS

The two-electron spherical tensor operator of Eq. (16) is now used to analyze the observed static exchange contributions to the zero-field exchange splittings discussed in Sec. III. As we have shown in Sec. II B. 1 it is sufficient to consider only the  $\Gamma_{00}^{00}$  and  $\Gamma_{00}^{20}$  terms in the exchange operator of Eq. (16), since the  ${}^8S_{7/2}$  and  ${}^6P_J$  states of  $\text{Gd}^{3+}$  in  $\text{GdCl}_3$  can be considered essentially pure. In addition, off-diagonal matrix elements give no significant contribution in the present analysis. The splittings are therefore a first-order effect, and the observed values of  $\Delta E_{\text{static}}$  may be directly equated to  $2W^\mu$  as we have shown in Sec. II A.

The diagonal matrix elements  $W^\mu$  defined by Eq. (7) were evaluated for the exchange operator of Eq. (16) using spherical tensor operator methods<sup>3,7</sup>

and the  $\text{Gd}^{3+}$  wave functions.<sup>18</sup> The coefficients of the  $\Gamma_{00}^{00}$  and  $\Gamma_{00}^{20}$  contributions are given in Tables III and IV with the factor of 2 from Eq. (14) included.

Since the static exchange splittings  $\Delta E_{\text{static}}$  depend linearly on the two-electron exchange parameters  $\Gamma_{00}^{00}$  and  $\Gamma_{00}^{20}$ , a standard least-squares-fitting procedure was used. Each level was assigned a weight of  $1/\sigma^2$  where  $\sigma$  is the uncertainty in  $\Delta E_{\text{static}}$ . The results of the fit are shown in the last column of Table II, where they may be compared with the observed static exchange contributions.

It can be seen that the two parameter exchange operator provides a reasonable description of the static exchange contributions to the  ${}^6P$  level splittings. Only the  ${}^6P_{7/2}$ ,  $M_J = \pm \frac{1}{2}$  state shows a difference slightly in excess of the experimental error. The two-electron exchange parameters resulting from the fit are

$$\left\{ \sum \Gamma_{00}^{00} \right\} = 2\Gamma_{00}^{00}(\text{nn}) + 6\Gamma_{00}^{00}(\text{nnn}) = 0.9 \pm 0.1 \text{ cm}^{-1} \quad (30)$$

and

$$\left\{ \sum \Gamma_{00}^{20} \right\} = 2\Gamma_{00}^{20}(\text{nn}) + 6\Gamma_{00}^{20}(\text{nnn}) = 0.1 \pm 0.6 \text{ cm}^{-1}. \quad (31)$$

They represent the total static exchange contribution of all interacting neighbors, generally assumed to be only the two nearest and six next-nearest neighbors.

One of the major goals of this study was to demonstrate that the same two-electron parameters are applicable to both ground and highly excited states. Success in this respect for  $\text{GdCl}_3$  is confirmed by a comparison of the isotropic parameter determined from the excited-state optical data with the corresponding parameter determined from high-frequency susceptibility studies of the ground state by Clover and Wolf.<sup>14</sup> They determined the nearest and next-nearest-neighbor exchange parameters,  $J_{\text{nn}} = -0.271 \pm .0014 \text{ cm}^{-1}$  and  $J_{\text{nnn}} = 0.0333 \pm 0.0014 \text{ cm}^{-1}$ , using the exchange Hamiltonian appropriate for the ground state, which in more conventional notation is given by

TABLE III. Contributions of the  $\Gamma_{00}^{00}$  and  $\Gamma_{00}^{20}$  terms of the two-electron spherical tensor operator to the static exchange splitting  $\Delta E_{\text{static}}$  for the experimentally observed  ${}^6P_J$  levels.

	${}^6P_{7/2} \frac{7}{2}$	${}^6P_{7/2} \frac{5}{2}$	${}^6P_{7/2} \frac{1}{2}$	${}^6P_{5/2} \frac{1}{2}$	${}^6P_{3/2} \frac{1}{2}$
$\Gamma_{00}^{00}$ coefficient	4.506	3.218	0.643	0.829	1.329
$\Gamma_{00}^{20}$ coefficient	1.478	0.019	-0.203	0.226	0.101

TABLE IV. Contributions of the  $\Gamma_{00}^{00}$  and  $\Gamma_{00}^{20}$  terms of the two-electron spherical tensor operator to the static exchange splitting  $\Delta E_{\text{static}}$  for  ${}^6P_J$  levels which were not observed.

	${}^6P_{7/2} \frac{3}{2}$	${}^6P_{5/2} \frac{5}{2}$	${}^6P_{5/2} \frac{3}{2}$	${}^6P_{3/2} \frac{3}{2}$
$\Gamma_{00}^{00}$ coefficient	1.931	4.147	2.488	3.988
$\Gamma_{00}^{20}$ coefficient	-0.402	-2.156	0.024	0.566

$$\mathcal{H}_{\text{exch}} = -2\vec{S}_i \cdot \vec{S}_j. \quad (32)$$

The exchange parameter  $J$  is related to the two-electron exchange integrals  $\mathcal{J}(m_a m_b; m'_a m'_b)$  by

$$J = \frac{1}{49} \sum_{m_a m_b} \mathcal{J}(m_a m_b; m_a m_b). \quad (33)$$

When the isotropic exchange parameter  $\Gamma_{00}^{00}$  in the spherical tensor operator notation is related to the  $\mathcal{J}$ 's through Eq. (17), it is found that

$$\Gamma_{00}^{00} = 7J. \quad (34)$$

Since our measured isotropic two-electron exchange parameter is the sum of contributions from all important neighbors, we must compare

$$\left\{ \sum \Gamma_{00}^{00} \right\} = 0.9 \pm 0.1 \text{ cm}^{-1},$$

with

$$7(2J_{\text{nn}} + 6J_{\text{nnn}}) = 1.0 \pm 0.1 \text{ cm}^{-1}. \quad (35)$$

It is quite significant that the excited-state and ground-state two-electron isotropic exchange parameters are, within experimental error, in complete agreement, as this demonstrates the ability of the two-electron tensor operator approach to *relate* exchange effects in various widely separated states such as the ground state and the highly excited  ${}^6P_J$  states at over 30 000  $\text{cm}^{-1}$ . This represents the first demonstration in rare-earth insulators that the same two-electron parameters are universally applicable to a wide range of states within a configuration.

Strong conclusions regarding the anisotropic exchange contribution to the  ${}^6P$  static level splittings unfortunately cannot be made on the basis of the present analysis. The relatively large uncertainty for the  $\Gamma_{00}^{20}$  parameter given in Eq. (31) is the result of both the experimental uncertainties in  $\Delta E_{\text{static}}$  and somewhat smaller coefficients<sup>33</sup> for the  $\Gamma_{00}^{20}$  parameter than for the  $\Gamma_{00}^{00}$  parameter, as shown in Table III. Obtaining a better determination of its value for this system would thus require either a dramatic improvement in experimental accuracy, which is not possible with the present

technique due to problems discussed in Sec. III, or a search for other levels which are more sensitive to its value. For completeness, coefficients of  $\Gamma_{00}^{00}$  and  $\Gamma_{00}^{20}$  are given in Table IV for  ${}^6P$  levels which could not be observed. Examination of Tables III and IV reveals that the largest  $\Gamma_{00}^{20}$  coefficient for states in the  ${}^6P$  manifold occurs for the  ${}^6P_{5/2}, M_J = \pm \frac{5}{2}$  level whose splitting was not observable by either electric dipole or magnetic dipole transitions from the ground state  ${}^8S_{7/2}, M_J = -\frac{7}{2}$  as pointed out in Sec. III. For neither that level nor for the  ${}^6P_{7/2}, M_J = \pm \frac{7}{2}$  level should the  $\Gamma_{00}^{20}$  contribution be regarded as negligible on the basis of present evidence.<sup>34</sup>

It is possible that further information regarding  $\Gamma_{00}^{20}$  could be obtained from the higher-lying  ${}^6I$  and  ${}^6D$  manifolds; however, at present we have chosen to study it and other anisotropic terms by exploring  $\text{Gd}^{3+}$  interactions with rare-earth impurity ions in  $\text{GdCl}_3$ . Preliminary studies of  $\text{Er}^{3+}$  impurity level splittings do indicate that higher rank anisotropic terms are important.<sup>13</sup>

Examination of Tables III and IV indicates a possible dramatic reduction in the number of parameters required for the application of the fundamental spherical tensor operator method to other systems. The coefficients of the  $\Gamma_{00}^{20}$  parameter vary from level to level by over two orders of magnitude, indicating that it may be reasonable to ignore some terms in more complicated systems after calculating the appropriate coefficients and estimating which terms seem unimportant.<sup>33</sup> Consistency of the results would then provide a check of the assumptions. Indeed in the present system, the  ${}^6P_{7/2}, M_J = \pm \frac{5}{2}$  splitting provides essentially a direct determination of the  $\Gamma_{00}^{00}$  parameter since the  $\Gamma_{00}^{20}$  coefficient is only 0.3% as large as the  $\Gamma_{00}^{00}$  coefficient for that level.<sup>33</sup> Further study of this point is certainly warranted.

## V. CONCLUSIONS

The fundamental two-electron tensor operator description of the electronic exchange interaction has been applied to the measured exchange splittings of  $\text{Gd}^{3+}$  in  $\text{GdCl}_3$  and the appropriate two-electron exchange parameters have been determined. It was shown that for ions occurring in large concentrations, such as the present case of  $\text{Gd}^{3+}$  in pure  $\text{GdCl}_3$ , a proper analysis of experimental exchange splittings requires that dynamic or transfer-of-energy contributions be considered in isolating the static exchange contributions.

From an analysis of the selection rules on the various possible mechanisms for the exchange splittings and a consideration of the composition of the five observed  ${}^6P$  states of  $\text{Gd}^{3+}$ , it was

shown that only the magnetic dipole-dipole and exchange interactions can contribute significantly. Using the  $Gd^{3+}$  wave functions and the symmetry properties of  $GdCl_3$ , the form of the two-electron tensor operator for the exchange interaction was obtained, and it was found that only the isotropic term  $\Gamma_{00}^{00}$  and one anisotropic term  $\Gamma_{00}^{20}$  contribute significantly to the static terms. The contributions due to dynamic exchange and the magnetic dipole-dipole interaction were determined and removed from the total observed exchange splittings, thus isolating the static contributions for the five observed states. These were then analyzed using the two-electron tensor operator which is applicable to *all* observed states. The two fitted parameters reproduce, within experimental uncertainty, the five observed exchange splittings.

The work reported here is part of a continuing series of studies whose major goal is to elucidate the nature of interactions and to improve the fundamental description of them in rare-earth and transition-metal insulators. Thus we will now explore how these results fit in with our more general goals.

First, the agreement between theory and experiment both in the present study of static exchange splittings and the earlier study of exciton dispersion<sup>4</sup> demonstrates that the two-electron description of the exchange interaction of Eqs. (15) and (16) (which we again emphasize are equivalent) provides an adequate description of the exchange interaction for rare-earth insulators. Second, and equally important, the agreement between the isotropic exchange parameter determined from excited-state optical data in the present study and that obtained from high-frequency susceptibility studies of the ground state properties<sup>14</sup> of  $GdCl_3$  demonstrates that this description of the exchange interaction is fundamental in the sense that the same two-electron parameters are applicable to dramatically different multielectron states separated in energy by as much as  $30\,000\text{ cm}^{-1}$ .

A third goal involves determination of the relative importance of the many anisotropic exchange terms. The  $\Gamma_{00}^{20}$  anisotropic parameter was unfortunately not well determined in the present study; however, its calculated coefficients indicate that it possibly makes important contributions to the splittings of selected  $^6P$  levels. The anisotropic  $\Gamma_{1-1}^{11}$  and  $\Gamma_{00}^{11}$  terms determined earlier<sup>4</sup> are quite comparable to the isotropic  $\Gamma_{00}^{00}$  term and give rise to exciton dispersions of up to  $2\text{ cm}^{-1}$  for  $^6P$  states in  $GdCl_3$  and  $Gd(OH)_3$ . As described elsewhere,<sup>35,36</sup> these same anisotropic terms are

responsible for observable anisotropic effects in the ground state  $^8S_{7/2}$  splittings of  $Gd^{3+}$  pairs in  $Y(OH)_3$  and  $Eu(OH)_3$ .

A further goal is the discovery of simplifications which can reasonably be made in the number of parameters to enable this approach to be applied to a wider class of systems. The large variation in the size of calculated coefficients of the  $\Gamma_{00}^{20}$  parameter (0.019–2.2) indicates that its contribution is negligible for some levels. This indicates that some terms allowed by symmetry may be reasonably neglected for some levels on the basis of calculated tensor operator matrix elements. These calculations may be readily programmed for a computer, so that a wide-ranging examination of the coefficients is feasible.

Finally, the ultimate goal of these studies of the exchange interaction is the demonstration that the same or very slightly adjusted two-electron exchange parameters are applicable to different rare-earth ions in related systems. The results of the present study combined with an analysis of  $Nd^{3+}$  and  $Er^{3+}$  impurity level splittings in  $^{13}GdCl_3$  indicate that the two-electron isotropic exchange parameters for  $Nd^{3+}$ - $Gd^{3+}$ ,  $Gd^{3+}$ - $Gd^{3+}$ , and  $Er^{3+}$ - $Gd^{3+}$  interactions show a slow, smooth, systematic variation over this sequence of ions which spans over two-thirds of the rare-earth series. Such a smooth variation is consistent with a slow change in the spatial extent of the  $4f$  wave functions, and indeed the apparent decreasing trend<sup>13</sup> for  $\{\sum \Gamma_{00}^{00}\}$  from  $Nd^{3+}$  to  $Gd^{3+}$  to  $Er^{3+}$  is just what would be expected on the basis of tighter binding for increasing atomic number. In addition, the anisotropic parameter  $\{\sum \Gamma_{00}^{20}\} = -0.2 \pm 0.2\text{ cm}^{-1}$  obtained from the  $Er^{3+}$  splittings in  $GdCl_3$  is, within experimental uncertainty, consistent with that obtained in the present study,  $\{\sum \Gamma_{00}^{20}\} = 0.1 \pm 0.6\text{ cm}^{-1}$ . Thus it may be that with further development the two-electron spherical tensor operator method can play a similar universal role in the description of the interionic exchange interaction to that of crystal field theory in the description of the single-ion energy levels of solids.

#### ACKNOWLEDGMENTS

The authors wish to express their appreciation to Dr. H. M. Crosswhite for the  $GdCl_3$  crystals used in this study, to Professor Werner P. Wolf, Professor P. M. Levy, and Professor M. F. Thorpe for helpful discussions, and to Tom Lynch for his assistance with the measurements.

- <sup>†</sup>Research supported by NSF Grant No. GH-43934.  
<sup>\*</sup>Present address.
- <sup>1</sup>W. P. Wolf, *J. Phys. (Paris)*, Colloq. **32**, C1-26 (1971).  
<sup>2</sup>J. M. Baker, *Rep. Prog. Phys.* **34**, 109 (1971).  
<sup>3</sup>R. L. Cone and W. P. Wolf, *AIP Conf. Proc.* **10**, 1039 (1973); *Phys. Rev. B* (to be published).  
<sup>4</sup>R. L. Cone and R. S. Meltzer, *Phys. Rev. Lett.* **30**, 859 (1973).  
<sup>5</sup>R. J. Birgeneau, *J. Chem. Phys.* **50**, 4282 (1969).  
<sup>6</sup>N. L. Huang, *Phys. Rev. B* **1**, 945 (1970).  
<sup>7</sup>P. M. Levy, *Phys. Rev.* **177**, 509 (1969).  
<sup>8</sup>R. J. Elliott and M. F. Thorpe, *J. Appl. Phys.* **39**, 802 (1968).  
<sup>9</sup>These "two-electron" exchange integrals are generally assumed to contain contributions from both direct exchange and superexchange processes.  
<sup>10</sup>P. M. Levy, *Phys. Rev.* **135**, A155 (1964).  
<sup>11</sup>E. Orlich and S. Hüfner, *Z. Phys.* **232**, 418 (1970).  
<sup>12</sup>J. R. Dean, D. Bloor, G. M. Copland, and V. Sells, *AIP Conf. Proc.* **5**, 259 (1972).  
<sup>13</sup>R. S. Meltzer, D. K. Braswell, and R. L. Cone, *AIP Conf. Proc.* **24**, 211 (1975).  
<sup>14</sup>R. B. Clover and W. P. Wolf, *Solid State Commun.* **6**, 331 (1968).  
<sup>15</sup>M. J. M. Leask, *J. Appl. Phys.* **39**, 908 (1968).  
<sup>16</sup>R. S. Meltzer and H. W. Moos, *Phys. Rev. B* **6**, 264 (1972).  
<sup>17</sup>The site symmetry of  $\text{GdCl}_3$  allows admixture of states in the  $M_J$  representation differing by  $\pm 6$ . Ignoring mixing between  $J$  manifolds, mixing can take place only within the  $J = \frac{7}{2}$  manifold for the pairs  $M_J = \pm \frac{7}{2}$ ,  $M_J = \pm \frac{5}{2}$ . This becomes important at high fields for  $M_J = +\frac{7}{2}$  and  $M_J = -\frac{5}{2}$ .  
<sup>18</sup>B. G. Wybourne, *Phys. Rev.* **148**, 317 (1966). Similar unpublished wave functions were obtained from H. M. Crosswhite.  
<sup>19</sup>R. L. Schwiesow and H. M. Crosswhite, *J. Opt. Soc. Am.* **59**, 592 (1969).  
<sup>20</sup>Each component of a single-ion Kramers doublet is regarded as a separate single-ion state here. Thus, each Kramers doublet gives four exciton levels.  
<sup>21</sup>In  $\text{GdCl}_3$   $V_{11} = V_{22}$  and  $V_{21} = V_{12}$ .  
<sup>22</sup>Spin selection rules on the energy-transfer matrix elements require that  $|\Delta S_z| \leq 1$ . For transfer between an ion in the ground state ( $S_z = -\frac{7}{2}$ ) and an ion in the upper Kramers component of an excited state ( $S_z = \frac{1}{2}$ ), this selection rule cannot be satisfied except for  $^6P$ ,  $J = \frac{7}{2}$ ,  $M_J = \frac{7}{2}$  component which mixes with  $M_J = -\frac{5}{2}$  at high fields; but even here the effect is negligible.  
<sup>23</sup>R. L. Cone and R. S. Meltzer, *J. Chem. Phys.* **62**, 3573 (1975).  
<sup>24</sup>K. B. Lyons, R. J. Birgeneau, E. I. Blount, and L. G. van Uitert, *Phys. Rev. B* **11**, 891 (1975).  
<sup>25</sup>J. W. Allen, R. M. Macfarlane, and R. L. White, *Phys. Rev.* **179**, 523 (1969) and R. M. Macfarlane and J. W. Allen, *Phys. Rev. B* **4**, 3054 (1971).  
<sup>26</sup>R. S. Meltzer, *Phys. Rev. B* **2**, 2398 (1970).  
<sup>27</sup>This definition is arbitrary and merely determines the normalization of the  $\Gamma_{qq}^{kk'}$  parameters. The  $u^{(k)}$  are even under inversion.  
<sup>28</sup>The energy-transfer matrix elements are under  $1 \text{ cm}^{-1}$  (see Ref. 4), whereas the manifolds of interest are separated by several hundreds of  $\text{cm}^{-1}$ .  
<sup>29</sup>These samples were grown by Earl Williams at Johns Hopkins University and were provided by H. M. Crosswhite.  
<sup>30</sup>W. P. Wolf, M. J. M. Leask, B. Mangum, and A. F. G. Wyatt, *J. Phys. Soc. Jpn. Suppl.* **17**, 487 (1961).  
<sup>31</sup>C. D. Marquard, *Proc. Phys. Soc. Lond.* **92**, 650 (1967).  
<sup>32</sup>R. I. Joseph and E. Schlömann, *J. Appl. Phys.* **36**, 1579 (1965).  
<sup>33</sup>Due to the somewhat arbitrary normalization vs  $k$  in the definition of Eq. (18), one must be cautious about comparing absolute values of  $\Gamma_{00}^{00}$  and  $\Gamma_{00}^{20}$  coefficients; however, it should be noted that the wider range of values for the  $\Gamma_{00}^{20}$  coefficients can be taken as evidence of less importance for that term for some levels.  
<sup>34</sup>Even if  $\{\sum \Gamma_{00}^{20}\}$  were quite small, one could not conclude that  $\Gamma_{00}^{20}(nn)$  and  $\Gamma_{00}^{20}(n\bar{n}\bar{n})$  individually were small as demonstrated by Eq. (35) where significant cancellation occurs due to  $J_{nn}$  and  $J_{n\bar{n}\bar{n}}$  having opposite signs. For some other phenomena the individual values rather than the summation are required.  
<sup>35</sup>R. W. Cochrane, C. Y. Wu, and W. P. Wolf, *Phys. Rev. B* **8**, 4348 (1973).  
<sup>36</sup>R. L. Cone, *Phys. Rev. B* (to be published).